An Evaluation of Media-Oriented Rate Selection Algorithm for Multimedia Transmission in MANETs

Mohammad Hossein Manshaei

Planète Project, INRIA, 2004 Route des Lucioles, B.P. 93, 06902 Sophia Antipolis Cedex, France
Email: manshaei@sophia.inria.fr

Thierry Turletti

Planète Project, INRIA, 2004 Route des Lucioles, B.P. 93, 06902 Sophia Antipolis Cedex, France
Email: turletti@sophia.inria.fr

Thomas Guionnet

Temics Project, IRISA-INRIA, Campus de Beaulieu, 35042 Rennes Cedex, France
Email: thomas.guionnet@irisa.fr

We focus on the optimization of real-time multimedia transmission over 802.11-based ad hoc networks. In particular, we propose a simple and efficient cross-layer mechanism that considers both the channel conditions and characteristics of the media for dynamically selecting the transmission mode. This mechanism called media-oriented rate selection algorithm (MORSA) targets loss-tolerant applications such as VoD that do not require full reliable transmission. We provide an evaluation of this mechanism for MANETs using simulations with NS and analyze the video quality obtained with a fine-grain scalable video encoder based on a motion-compensated spatiotemporal wavelet transform. Our results show that MORSA achieves up to 4 Mbps increase in throughput and that the routing overhead decreases significantly. Transmission of a sample video flow over an 802.11a wireless channel has been evaluated with MORSA. Important improvement is observed in throughput, latency, and jitter while keeping a good level of video quality.

Keywords and phrases: ad hoc networks, cross-layer optimization, IEEE 802.11 wireless LAN, MANETs, mode selection algorithms.

1. INTRODUCTION

With recent performance advancements in computer and wireless communications technologies, mobile ad hoc networks (MANETs) are becoming an integral part of communication networks. The emerging widespread use of real-time voice, audio, and video applications generates interesting transmission problems to solve over MANETs. Many factors can change the topology of MANETs such as the mobility of nodes or the changes of power level. For instance, power control done at the physical (PHY) layer can affect all other nodes in MANETs, by changing the levels of interference experienced by these nodes and the connectivity of the network, which impacts routing. Therefore, power control is not confined to the physical layer, and can affect the operation of higher-level layers. This can be viewed as an opportunity for cross-layering design and poses many new and significant challenges with respect to wired and traditional wireless networks. As soon as we want to optimize data transmission according to both the characteristics of the data and to the varying channel conditions, a cross-layering approach becomes necessary. Numerous cross-layer protocols have already been proposed in the literature [1, 2, 3, 4, 5]. They focus on the interactions between the application, transport, network, and link layers. With the recent interest on software radio designs [6], it becomes possible to make the PHY layer as flexible as the higher layers. Adaptive and cross-layering interactions can now affect the whole stack of the communication protocol. Consequently, the classical OSI approach of providing a PHY layer as reliable as possible

TABLE 1: Characteristics of the various physical layers in the IEEE 802.11 standard.

Characteristic	802.11a	802.11b	802.11g
Frequency	5 GHz	2.4 GHz	2.4 GHz
Rate (Mpbs)	6, 9, 12, 18, 24, 36, 48, 54	1, 2, 5.5, 11	1, 2, 5.5, 6, 9, 11, 12, 18, 22, 24, 33, 36, 48, 54
Modulation	BPSK, QPSK, 16 QAM, 64 QAM	DBPSK, QPSK, CCK	BPSK, DBPSK, QPSK, DQPSK, CCK
	OFDM	DSSS	16 QAM, 64 QAM (OFDM and DSSS)
FEC rate	1/2, 2/3, 3/4	NA	1/2, 2/3, 3/4
Basic rate	6 Mbps	1 Mbps or 2 Mbps	1, 2, or 6 Mbps

independently of the type of data transmitted becomes questionable.

In this paper, we focus on the optimization of realtime multimedia transmission over 802.11-based MANETs. In particular, we propose a simple and efficient cross-layer protocol which dynamically adjusts the transmission mode, that is, the physical modulation, rate, and possibly the forward error correction (FEC). This protocol called MORSA (media-oriented rate selection algorithm) is convenient for loss-tolerant (LT) applications such as video or audio codecs that do not require 100% transmission reliability (i.e., a certain level of packet error rate (PER) or bit error rate (BER) can be concealed at the receiver). Contrary to mail and file transfer applications, several multimedia applications, such as audio and video conferencing or video on demand (VoD) can tolerate some packet loss. For example, an MPEG video data flow can contain three different types of packet, intrapicture (I) frames, prediction (P) frames, and biprediction (B) frames. I-frames are more important for the overall decoding of the video stream, because they serve as reference frames for P- and B-frames. Therefore, the loss of an I-frame has a more drastic impact on the quality of the video playback than the loss of other types of frames. In this respect, the frame loss requirement of I-frames is more stringent than those of P- and B-frames. Furthermore, as described in Section 6, some multimedia applications implement their own error control mechanisms [7, 8], making it inefficient to provide full reliability at the link layer.

MORSA takes into account both the intrinsic characteristics of the application and varying conditions of the channel. It selects the highest possible transmission rate while guaranteeing a specific bit error rate: the selected transmission mode varies with time depending on the PER or BER tolerance and on the signal-to-noise ratio (SNR) measured at the receiver. We show in this paper that by adaptively selecting the transmission mode according to both loss tolerance requirements of the application and varying channel conditions, the application-layer throughput can be significantly increased and more stability can be achieved in ad hoc routing. Finally, we evaluate the quality of a sample video transmitted over a wireless 802.11a channel using MORSA and compare it with the quality obtained when we do not take into account characteristics of the application (i.e., using the standard approach). Our results show that MORSA can reach a comparable video quality than the one obtained with the standard mechanism while using only a very low (5%) FEC overhead at the application level instead of the physical layer

Sent with basic rate ⟵ Sent with the rate indicated in PLCP ⟶
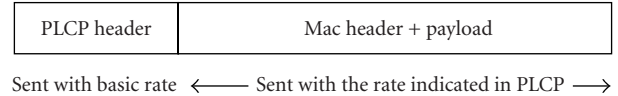
FIGURE 1: Data rates for packet transmission.

FEC (50% or 25%). This significantly decreases transmission delay of the application.

Throughout this paper, we assume that wireless stations use the enhanced distributed channel access (EDCA), proposed in the IEEE 802.11e [9] to support different levels of QoS. We have modified the NS simulation tool to evaluate the overall system efficiency when considering the interaction between layers in the protocol stack.

The rest of this paper is structured as follows. In Section 2, we overview the salient features of the MAC and PHY layers in the 802.11 schemes. We also review some of the automatic rate selection algorithms that were proposed in the literature. In Section 3, we present related work about cross-layer protocols in ad hoc networks. The MORSA scheme and a possible implementation within an 802.11 compliant device are discussed in Section 4. Simulation results with NS are analyzed in Section 5. We evaluate quality of a sample video transmission over a wireless channel in Section 6. Finally, the conclusion is presented in Section 7.

2. BACKGROUND

Today, three different PHY layers are available for the IEEE 802.11 WLAN as shown in Table 1.

The performance of a modulation scheme can be measured by its robustness against path loss, interferences, and fading that cause variations in the received SNR. Such variations also cause variations in the BER, since the higher the SNR, the easier it is to demodulate and decode the received bits. Compared to other modulations schemes, BPSK has the minimum probability of bit error for a given SNR. For this reason, it is used as the basic mode for each PHY layer since it has the maximum coverage range among all transmission modes. As shown in Figure 1, each packet may be sent with two different rates [10]: its PLCP (physical layer convergence protocol) header is sent at the basic rate while the rest of the packet might be sent at a higher rate. The higher rate, used to transmit the physical layer payload, which includes the MAC header, is stored in the PLCP header.

The receiver can verify that the PLCP header is correct (using CRC or Viterbi decoding with parity), and uses the transmission mode specified in the PLCP header to decode the MAC header and payload. The mode with the lowest rate is used to transmit the PLCP header. Transmission mode selection can be performed manually or automatically in each station. A number of rate selection algorithms have been proposed in the literature. They include the auto-rate fallback (ARF) [11], the receiver-based auto-rate (RBAR), [12] and MiSer [13] schemes. RBAR tries to select the best mode (i.e., the mode with the highest rate) based on the received SNR, while ARF uses a simple ACK-based mechanism to select the rate. MiSer is a protocol based on the 802.11a/h standards whose goal is to optimize the local power consumption. While all these automatic rate selection mechanisms try to adapt the transmission mode according to the channel conditions, we are not aware of any protocol that considers characteristics of the application.

Since MORSA is based on RBAR, we detail the latter here. In RBAR, the sender chooses a data rate based on some heuristic (e.g., the most recent rate that was used to successfully transmit a packet), and then stores the rate and the packet size into the request-to-send (RTS) control packet. Stations that receive the RTS can use the rate and packet size information to calculate the duration of the requested reservation. They update their network allocation vectors (NAVs) to reflect the reservation. While receiving the RTS, the receiver uses the current channel state as an estimate of the channel state when the upcoming packet is supposed to be transmitted. The receiver then selects the appropriate rate with a simple threshold-based mechanism and includes this rate (along with the packet size) in a clear-to-send (CTS) control packet. Stations that overhear the CTS calculate the duration of the reservation and update their NAVs accordingly. Finally, the sender responds to the CTS by transmitting the data packet at the rate selected by the receiver. Note that nodes that cannot hear the CTS can update their NAVs when they overhear the actual data packet by decoding a part of the MAC header called the *reservation subheader*. Further information concerning RBAR, including implementation and performance issues in 802.11b, is available in [12].

3. RELATED WORK

Several cross-layer mechanisms such as mechanisms for TCP over wireless links [1, 5], power control [14], medium access control [2], QoS providing [15], video streaming over wireless LANs [16], and deployment network access point [1] have been proposed.

The Mobileman European Project [17] introduced inside the layered architecture the possibility that protocols belonging to different layers can cooperate by sharing network status information while still maintaining separation between the layers in protocol design. The authors propose applying triggers to the network status such that it can send signals between layers. In particular, This cross-layering approach addresses the security and cooperation, energy management, and quality-of-service issues.
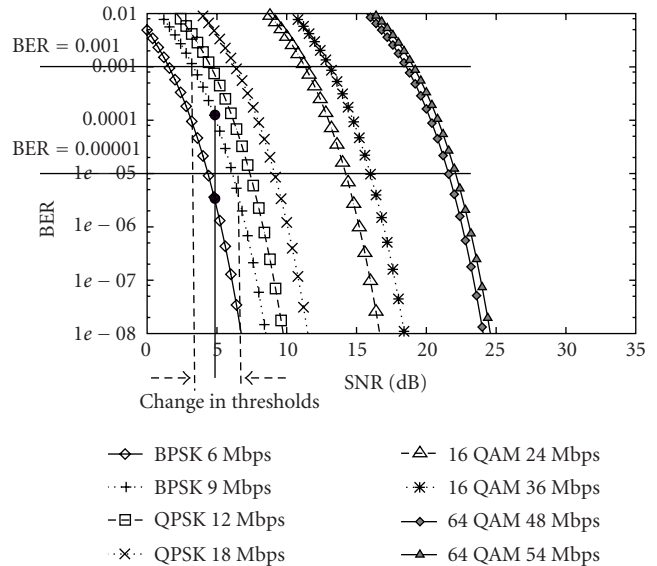

Figure 2: BER versus SNR for various transmission modes (802.11a).

The effect of such cross-layer mechanisms on the routing protocol, the queuing discipline, the power control algorithm, and the medium access control layer performance have been studied in [2].

A cross-layer algorithm using MAC channel reservation control packets at the physical layer is described in [4]. This mechanism improves the network throughput significantly for mobile ad hoc networks because the nodes are able to perform an adaptive selection of a spectrally efficient transmission rate.

Reference [16] describes a cross-layer algorithm that employs different error control and adaptation mechanisms implemented on both application and MAC layers for robust transmission of video. These mechanisms are media access control (MAC) retransmission strategy, application-layer forward error correction (FEC), bandwidth-adaptive compression using scalable coding, and adaptive packetization strategies. Similarly a set of end-to-end application-layer techniques for adaptive video streaming over wireless networks is proposed in [18]. In [19], the adaptive source rate control (ASRC) scheme is proposed to adjust the source rate based on the channel conditions, the transport buffer occupancy, and the delay constraints. This cross-layer scheme can work together with hybrid ARQ error control schemes to achieve efficient transmission of real-time video with low delay and high reliability. However, none of these algorithms have tried to adapt the physical layer transmission mode in 802.11 WLANs. More examples could be cited, but we are not aware of any cross-layer algorithm that takes into account the physical layer parameters (e.g., PHY FEC) as explained in Section 2.

It should be noted that standardization efforts are in progress to integrate various architectures. The important codesign of the physical, MAC, and higher layers have been taken into account in some of the latest standards like

TABLE 2: SNR (dB) threshold values to select the best transmission mode.

PHY Rate	Standard (with FEC)	Media-oriented (no LT)	Media-oriented (0.1% LT)
12 Mbps	0.68	6.12	4.94
18 Mbps	4.75	7.37	6.18
36 Mbps	11.39	14.22	13.5
54 Mbps	17.29	21.58	20.3

TABLE 3: Loss tolerance classification.

Bits 6-7	Application sensitivity
00	No tolerance in payload
01	Low loss tolerance in payload
10	Medium loss tolerance in payload
11	High loss tolerance in payload

3G standards (CDMA2000), BRAN HiperLAN2, and 3GPP (high-speed downlink packet access) [1]. IEEE has also considered a cross-layer design in the study group on mobile broadband wireless access (MBWA).

4. CROSS-LAYER MODE SELECTION PROTOCOL

This section describes the MORSA mechanism and discusses implementation issues.

4.1. Algorithm description

As we already mentioned, real-time multimedia applications can be characterized by their tolerance to a certain amount of packet loss or bit errors. These losses can be ignored (if they are barely noticeable by human viewers) or compensated at the receiver using various error concealment techniques. In our scheme, the sender is able to specify its loss tolerance (LT) such that the receiver uses both this information and the current channel conditions to select the appropriate transmission mode (i.e., rate, modulation, and FEC level). More precisely, the sender includes the LT information in each RTS packet to allow the receiver to select the best mode. The LT information is also included in the header of each data packet such that the receiver can decide whether or not to accept a packet. While receiving the RTS, the receiver uses the information concerning the channel conditions along with the information related to LT to select the best data rate for the corresponding packet. The selected rate is then transmitted along with the packet size in the CTS back to the sender, and the sender uses this rate to send its data packets. When a packet arrives at the receiver side, if the receiver is able to decode the PLCP header, it can identify the BER tolerance for the encoded payload. If the packet can tolerate some bit errors, it has to be accepted even if its payload contains errors. As will be shown later, our mechanism makes it possible to define new transmission modes that do not use FEC but that exhibit comparable throughput performance.

To take into account both the SNR and the LT information, we have modified the RBAR threshold[1] mechanism. For 802.11a, we assume that the receiver uses FEC Viterbi decoding. The upper bound on the probability of error provided in [13, 20] is used under the assumption of binary convolutional coding and hard-decision Viterbi decoding. Specifically, for a packet of length L (bytes), the probability of packet error can be bound by

$$P_e(L) \leq 1 - (1 - P_u)^{8L}, \qquad (1)$$

where the union bound P_u of the first-event error probability is given by

$$P_u = \sum_{d=d_{\text{free}}}^{\infty} a_d \cdot P_d \qquad (2)$$

with d_{free} the free distance of the convolutional code, a_d the total number of error events of weight[2] d, and P_d the probability that an incorrect path at distance d from the correct path is chosen by the Viterbi decoder. When hard-decision decoding is applied, P_d is given by (3), where ρ is the probability of bit error for the modulation selected in the physical layer.[3]

$$P_d = \begin{cases} \sum_{k=(d+1)/2}^{d} \binom{d}{k} \cdot \rho^k \cdot (1-\rho)^{d-k} & \text{if } d \text{ is odd,} \\ \frac{1}{2} \cdot \binom{d}{d/2} \cdot \rho^{d/2} \cdot (1-\rho)^{d/2} & \text{if } d \text{ is even,} \\ + \sum_{k=d/2+1}^{d} \binom{d}{k} \cdot \rho^k \cdot (1-\rho)^{d-k}. \end{cases} \qquad (3)$$

Figure 2 shows an example of the modifications made for the SNR threshold in RBAR with and without the media-oriented mechanism. Commonly, a BER at the physical layer smaller than 10^{-5} is considered acceptable in wireless LAN applications. By using theoretical graphs of BER as function of the SNR for different transmission modes on a simple additive white Gaussian noise (AWGN) channel (see Figure 2), we can compute the minimum SNR values required. Now, if a particular application can tolerate some bit errors (e.g., a BER up to the 10^{-3} as shown in Figure 2), the receiver can select the highest rate for the following data transmission corresponding to this SNR. For example in Figure 2, when the SNR is equal to 5 dB, the receiver can select a 9 Mbps data rate instead of a 6 Mbps data rate if it is aware that the application can tolerate a BER less than 10^{-3}.

We have calculated the thresholds using (1), (2), and (3) for an application that can tolerate up to 10^{-3} BER (see

---

[1] These thresholds are used to select the best transmission mode in the receiver.

[2] We have used the a_d coefficients provided in [21].

[3] In this paper, we use additive white Gaussian noise (AWGN) channel model.

Bits 0–3	Bit 4	Bit 5	Bits 6-7	Bits 8–15
Traffic ID	*Schedule pending*	*ACK policy*	*Reserved*	*TXOP duration*

FIGURE 3: QoS control field in the 802.11e.

FIGURE 4: Modifications to the RTS header.

Table 2). The receiver can use arrays of thresholds that are precomputed for different LTs.

In the following sections, we describe how such a mechanism can be implemented in 802.11-based WLANs.

4.2. Implementation issues

We propose to implement MORSA with the help of the EDCA protocol [22, 23]. EDCA is one of the features that has been proposed by IEEE 802.11e to support QoS in WLANs [9]. In this protocol, each QoS-enhanced station (QSTA) has 4 queues to support up to 8 user priorities (UPs). Figure 3 shows the QoS control field that is added to the MAC header in the 802.11e specification [9]. Bits 6 and 7 of this header can be used to indicate the loss tolerance information. Table 3 shows a possible meaning for these two bits in our media-oriented mechanism that should be defined in the process of connection setup. LT information is sent to the receiver by adding one byte to the RTS packets as illustrated in Figure 4.

To make our mechanism operational, it is crucial to let the packets with corrupted payload reach the receiver's application layer. As such, some modifications of the standard are necessary. First, the CRC at the MAC layer should no more cover the payload but only the MAC, IP, UDP, and possibly the RTP headers. Second, the optional UDP checksum must be disabled, as described in the UDP lite proposal [24]. UDP lite is a lightweight version of UDP with increased flexibility in the form of a partial checksum. The coverage of the checksum is specified by the sending application on a per-packet basis. This protocol can be profitable for MORSA. Furthermore, to make our mechanism more robust against bit errors, the headers of the different layers (MAC, IP, UDP, and RTP) have to be sent with the basic rate (see Figure 5). This is somewhat similar to the reservation subheader used in [12] as explained in Section 2. The corresponding bandwidth overhead is investigated in the next section.

5. SIMULATION RESULTS

Our simulations are based on the simulation environment described in [25] which uses the NS-2 network simulator, with extensions from the CMU Monarch Project [26] to simulate multihop wireless ad hoc networks. In order to obtain more realistic results, Cisco Aironet 1200 Series parameters

are used in our simulations [27]. Further details about the simulation environment are available in [25].

Note that in the following simulations, CTS and RTS control packets and PLCP headers are sent with a BPSK modulation, an FEC rate equal to 1/2, and a 6 Mbps data rate. All throughputs shown in the following figures exclude the MAC and PHY headers; they are denoted as goodputs for the remainder of the paper.

To evaluate the perceived quality for the user using our protocol, we have taken an example of video application that can tolerate 0.1% of bit errors (see Section 6.2). Thus, we have investigated the throughput performance of MORSA when the BER is equal to 10^{-3} in the following simulations. Of course other values of the BER can be chosen to perform simulations with similar results.

In our simulation, we assume that bit errors in a packet are distributed according to a binomial distribution. This is an acceptable assumption since the position of the bit errors are not taken into account by NS-2. In Section 6, we will provide more precise models for the distribution of bit errors in our data stream. Let n represent the number of bit errors in a packet of N bits, and let p be the probability of bit error. The probability of having less than L bit errors can be calculated by

$$P(n \leq L) = \sum_{i=0}^{L} \binom{N}{i} \cdot p^i \cdot (1-p)^{N-i}. \tag{4}$$

We first evaluate our mechanism in a simple ad hoc network that contains two wireless stations. These wireless stations communicate on a single channel. Station A is fixed and station B moves toward station A. Station B moves in 5 m increments over the range of mobility (0 m–200 m) and is held fixed for a 60s transmission of CBR data towards station A. In each step 30000 CBR packets of size 2304 bytes (including physical layer FEC) are sent.

Figure 6 shows the mean goodput of this single CBR connection between two wireless stations versus the distance between them for different transmission modes with and without media-oriented mechanism.[4]

Since no payload FEC is used in our media-oriented protocol, the mean goodput is increased significantly compared to the standard transmission modes. For example, we can observe that the media-oriented mechanism achieves a 4 Mbps mean goodput improvement at the highest rate mode. However, this has a cost in coverage range: in the same example,

---

[4]Based on our simulation study for 802.11a, we have selected five efficient transmission modes out of the 8 possible transmission modes in 802.11a [25].
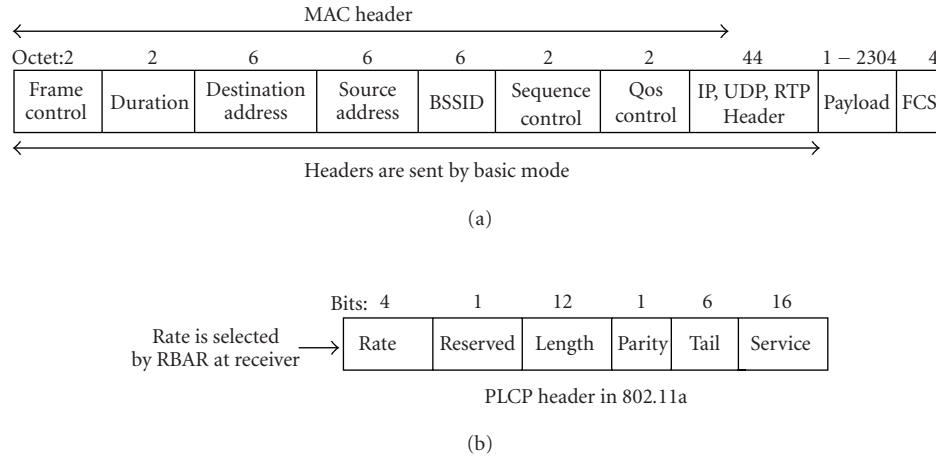
(a)

PLCP header in 802.11a
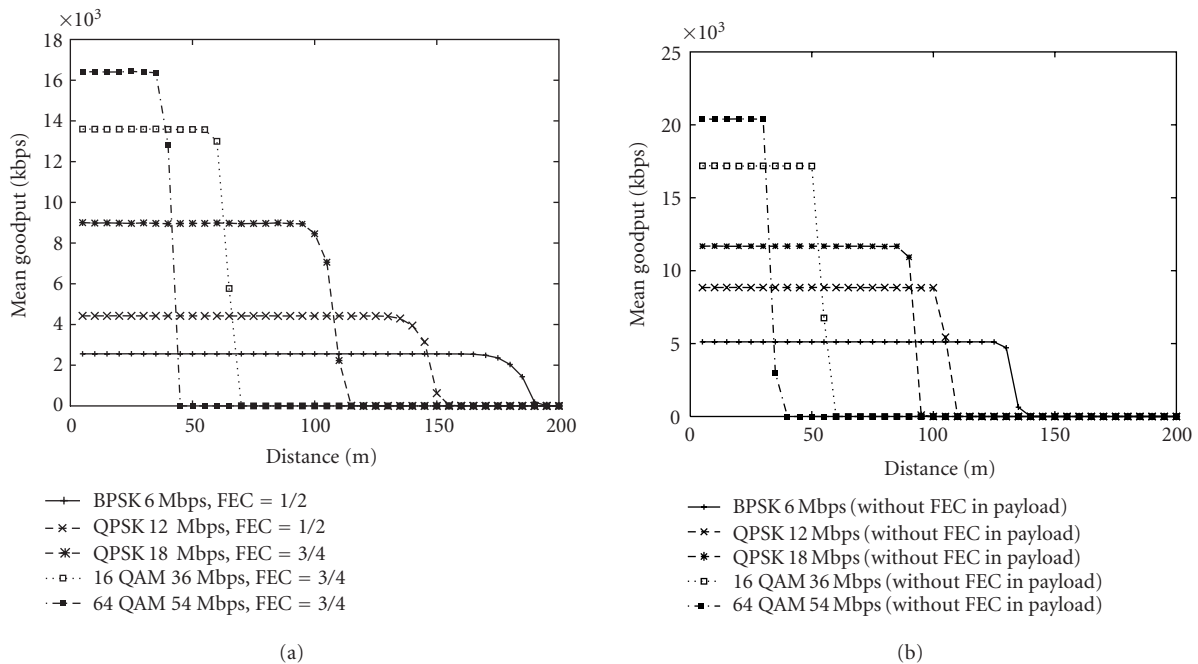
(b)

FIGURE 5: Proposed frame format.

FIGURE 6: (a) Mean goodput versus distance for standard transmission modes and (b) media oriented with 0.1% bit errors.

it is 50 meters less. It should be noted that if an application can tolerate more bit errors, the coverage range will be larger than for the standard transmission modes [23].

We have also evaluated the extra bandwidth overhead of the modified frame format. This overhead is caused by having to send the MAC header at the basic mode and by the additional byte in the RTS packet. Figure 7 compares the mean throughput for the traditional RBAR and for RBAR with the modified frame format. The worst-case overhead at the maximum rate is about 1 Mbps, but the coverage range does not change much compared to the standard specification.

To evaluate the performance of RBAR under different mode selection mechanisms, we need to calculate arrays of thresholds for each mechanism (see Section 4). Table 2 shows these threshold values for RBAR and MORSA.[5] These results show that if we can tolerate loss, we will be able to send data with a higher rate.

Figure 8 illustrates the performance of RBAR and MORSA. Since the standard mode selection mechanism

---

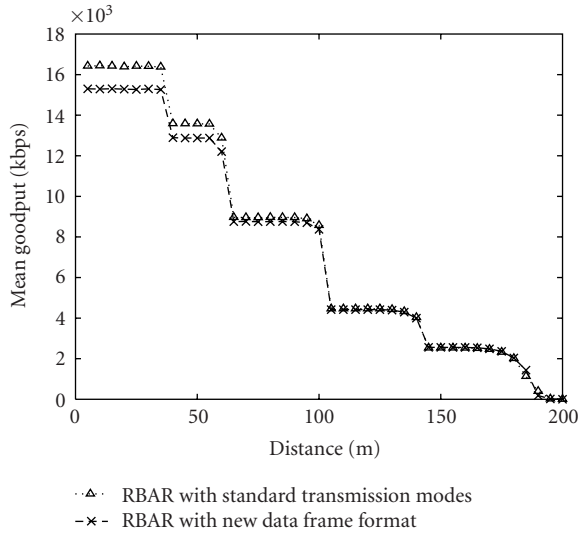[5]For an SNR smaller than these values, data will be sent with the basic mode which is 6 Mbps.

Figure 7: Overhead of the modified frame format.

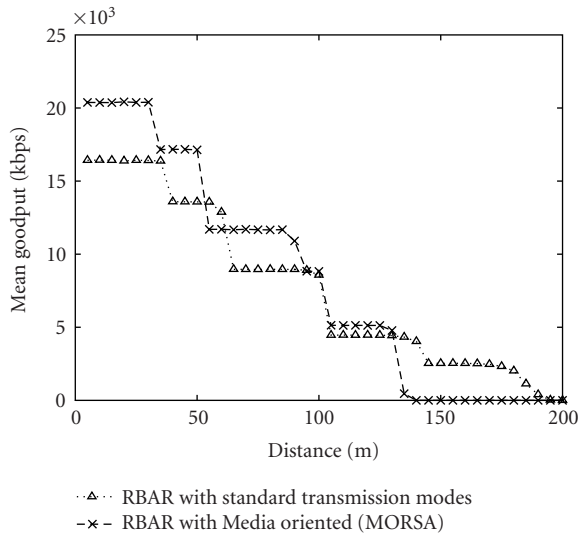Figure 8: RBAR performance for standard and media-oriented protocols (MORSA).

Figure 9: RBAR performance using standard or media-oriented protocol (H-MORSA).
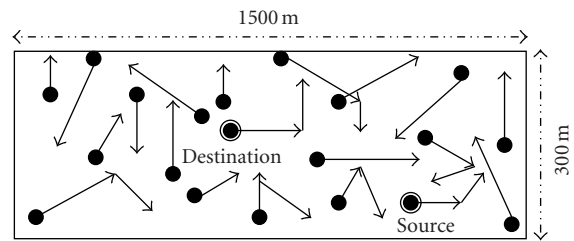
Figure 10: Example of ad hoc network topology scenario.

can achieve the maximum coverage range and the media-oriented mechanism obtains the maximum mean goodput, we have defined a new media-oriented mode selection mechanism called *hybrid transmission mode selection* or *H-MORSA*, to achieve both objectives at the same time (see Figure 9). The five PHY transmission modes that are used for the hybrid mode selection mechanism do not use FEC.

Then, we evaluate the two media-oriented mechanisms (MORSA and H-MORSA) in ad hoc networks. Figure 10 shows an example of network configuration for 20 nodes which are commonly used for ad hoc network evaluation [12, 26, 28].In our simulation, each ad hoc network consists of 20 mobile nodes that are distributed randomly in a 1500×300 meter arena. The speed at which nodes move is uniformly distributed between $0.9v$ and $1.1v$, for different
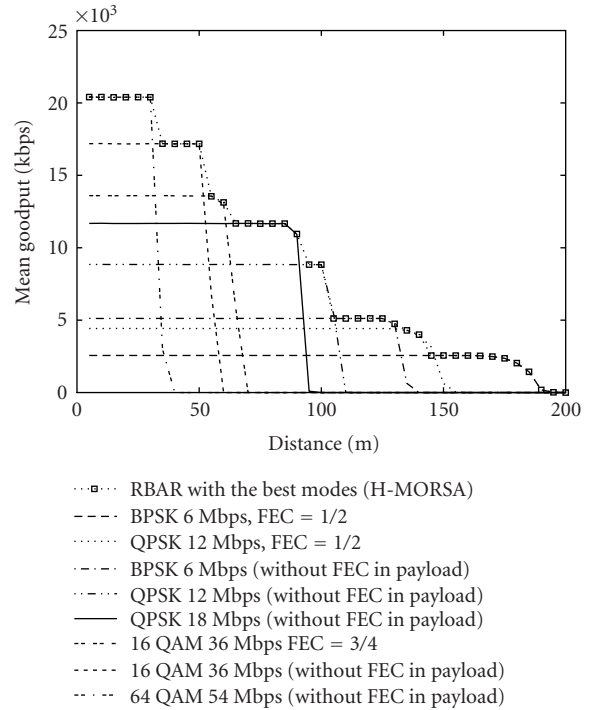
speeds of v. We use the following speed values 2, 4, 6, 8, and 10 m/s. The nodes choose their path randomly according to a random waypoint mobility pattern. The same movement patterns are used in all experiments whatever the mean node speed. For example, if node A moves from point a to point b with a speed of 2 m/s, it will take the same route with 4, 6, 8, and 10 m/s in the other scenario patterns but with different delays. All the results are based on an average over 30 simulations with 30 different scenario patterns.

In each simulation, a single UDP connection sends data between two selected nodes. Other nodes can forward their packets in the ad hoc network. The data is generated by a CBR source at saturated rate. In other words, there are always packets to send during the whole simulation time. Unlike in the simple network topology with 2 nodes where we used static routing, here the dynamic source routing (DSR) [28] protocol has been used. DSR is a simple and efficient
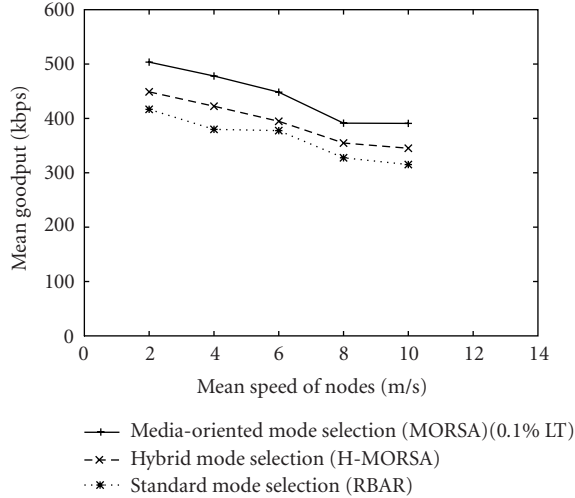
FIGURE 11: Performance comparison for a single CBR connection in a multihop network, with and without MORSA.
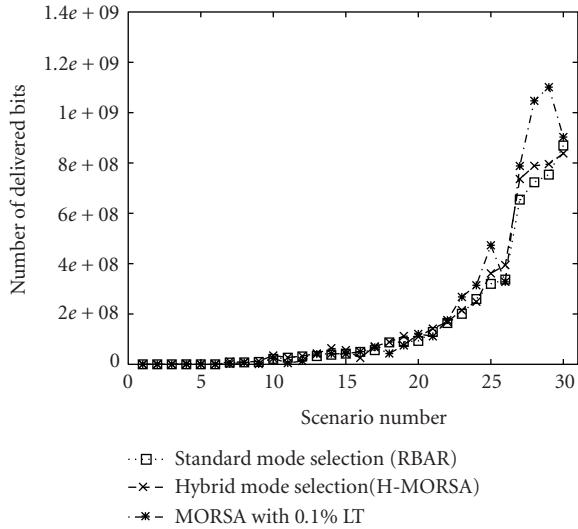

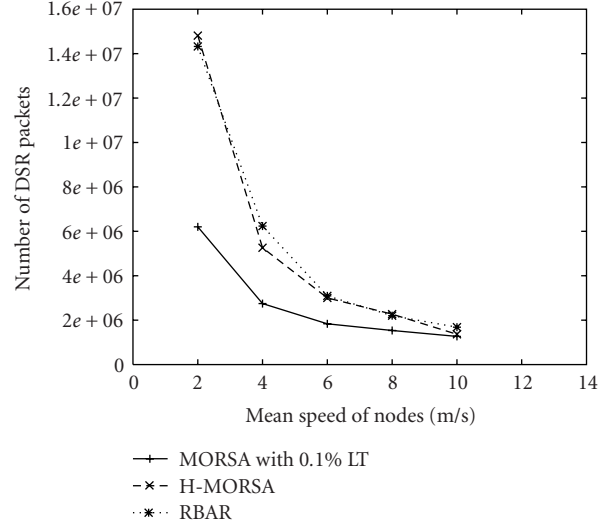FIGURE 12: Number of delivered bits to the application (speed = 2 m/s).
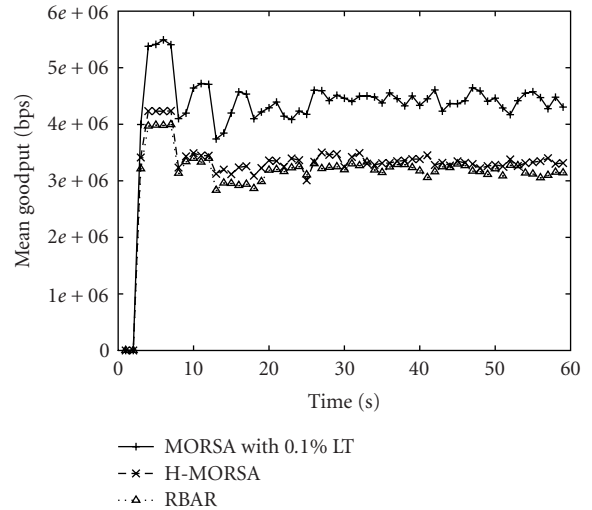

FIGURE 13: DSR routing overhead in multihop network.

FIGURE 14: Performance comparison for a several CBR connection in multihop network, with and without media-oriented mechanism.

routing protocol designed specifically for use in multihop ad hoc networks. It should be noted that routing packets are sent using the basic transmission mode like the RTS, CTS, and ACK control packets.

We use three automatic mode selection mechanisms defined in our previous simulations (see Figures 8 and 9). In the standard mode selection mechanism (RBAR) and hybrid mode selection mechanism (H-MORSA), we may have a hop in the route between source and destination that uses a physical FEC equal to 1/2. Thus, we have to use packets with a payload length equal to 1152 bytes for these simulations. However, with MORSA, we are able to send packets with 2304 bytes since no physical layer FEC is used in this mechanism.

Figure 11 shows the mean goodput of a single CBR connection versus different mean node speeds. For an application that can tolerate a BER of 10^{-3}, the mean goodput is about 25% higher when we take into account the application's characteristics.

Figure 12 shows the number of delivered bits for 30 scenario patterns[6] with mean speed equal to 2 m/s. In the scenarios where the number of delivered bits is zero, DSR was not able to find a route between the source and the destination during the whole simulation time. As expected, in most of the scenario patterns, MORSA can deliver more

---

[6]Scenarios are sorted by the number of delivered bits obtained with the standard mode selection mechanism.
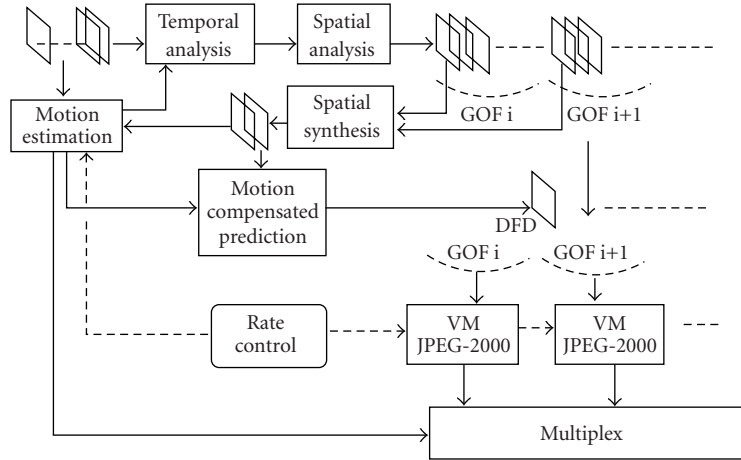
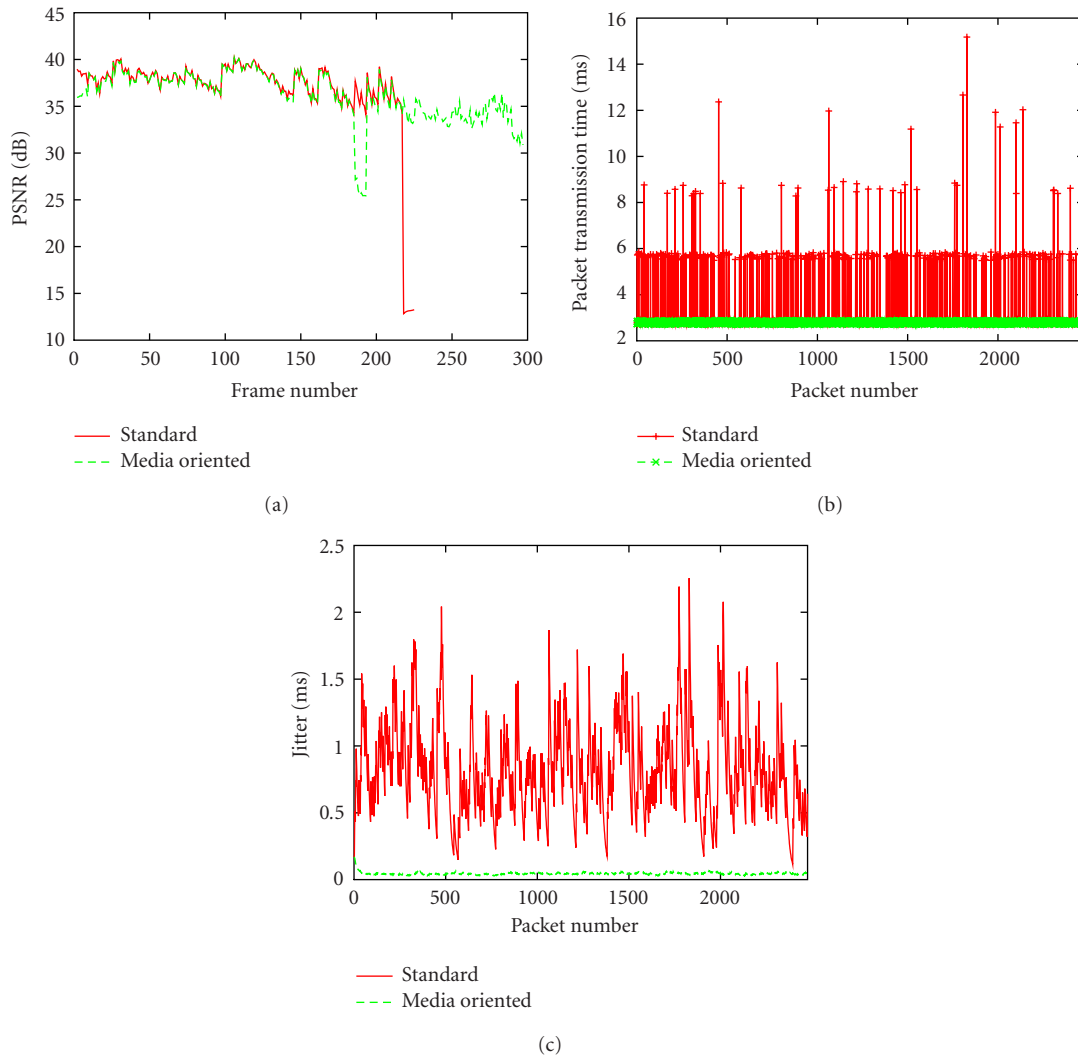FIGURE 15: WAVIX structure.

(a)

(b)

(c)

FIGURE 16: PSNR, transmission delay, and jitter comparison (SNR = −1.6 dB, 6 Mbps, FEC= 1/2, BPSK).

data bits to the receiver. One interesting observation is that in some scenario patterns (less than 15% of them), the number of delivered bits with the standard RBAR and H-MORSA is more than the one in MORSA. The rationale be-
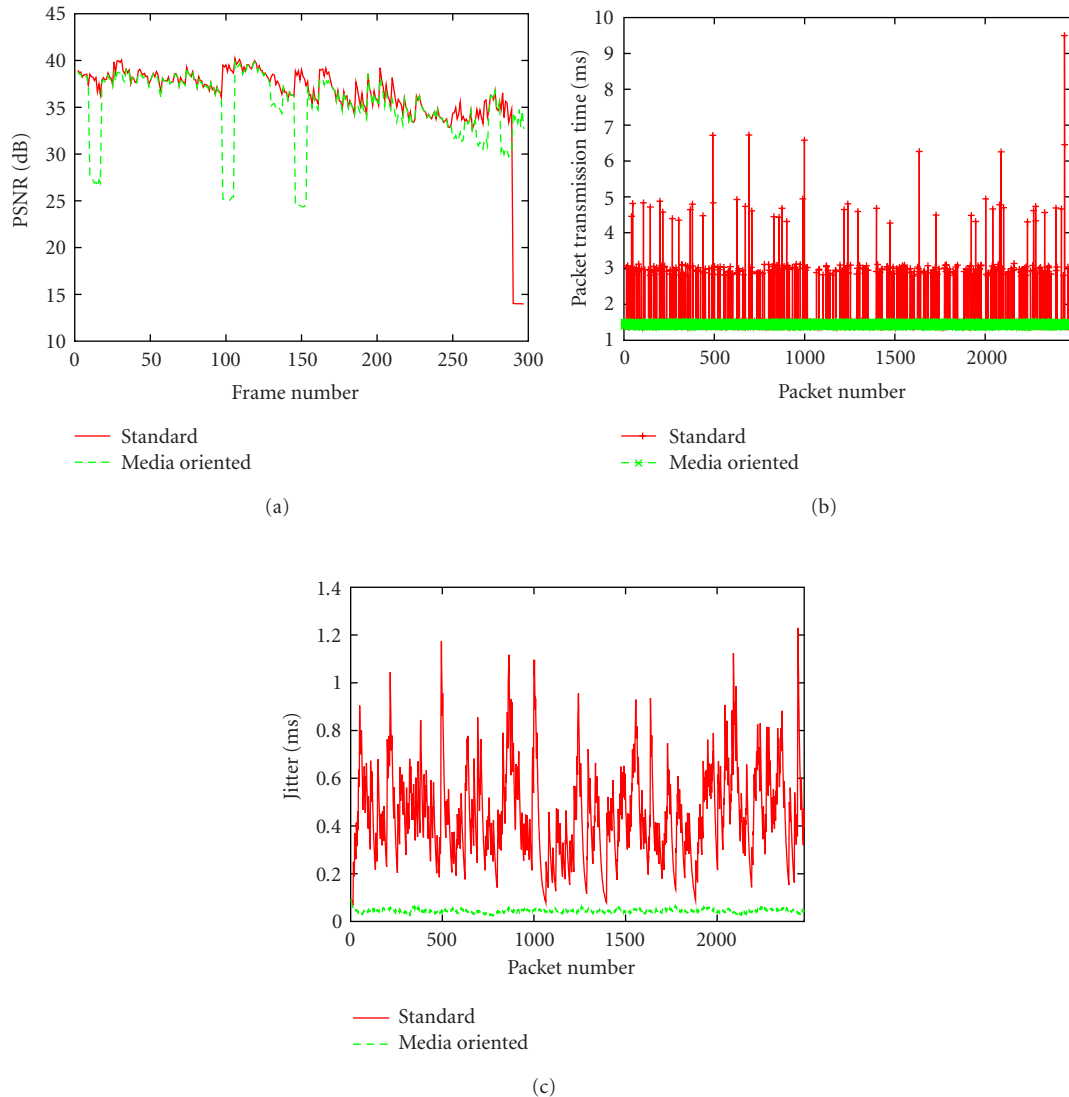
(a)

(b)

(c)

FIGURE 17: PSNR, transmission delay, and jitter comparison (SNR = 1.3 dB, 12 Mbps, FEC= 1/2, QPSK).

hind this is that DSR packets can be sent with the maximum coverage range in the standard and the hybrid mode selection mechanisms. As a result, the source can find a route to the destination faster than MORSA. Thus, the number of delivered packets in the standard RBAR and the H-MORSA is more than that of MORSA (e.g., scenario number 20).

We have also evaluated the overhead of the DSR routing protocol in different cases. The DSR algorithm has two different phases called *route discovery* and *route maintenance* to manage the routes in ad hoc networks. In *route discovery*, ad hoc nodes need to find a route between the source and the destination. This is performed only when the source attempts to send a packet to the destination and does not already know a route. In *route maintenance*, DSR detects changes in the network topology such that the

source can no longer use the current route to destination. This can occur if a link along the route is not usable anymore.

Figure 13 shows the number of routing overhead packets generated by DSR, which have been sent in ad hoc networks according to different mean speed of the nodes. In order to evaluate this overhead, we have considered all DSR routing packets that should be sent before making a connection and during data transmission. So this overhead includes *route discovery* and *route maintenance* overheads. These results show that routing overhead decreases significantly when we use MORSA. We believe this is a consequence of having more stable connection when MORSA is used.

We have done different simulations to evaluate the performance of our mechanism in the presence of interfer-
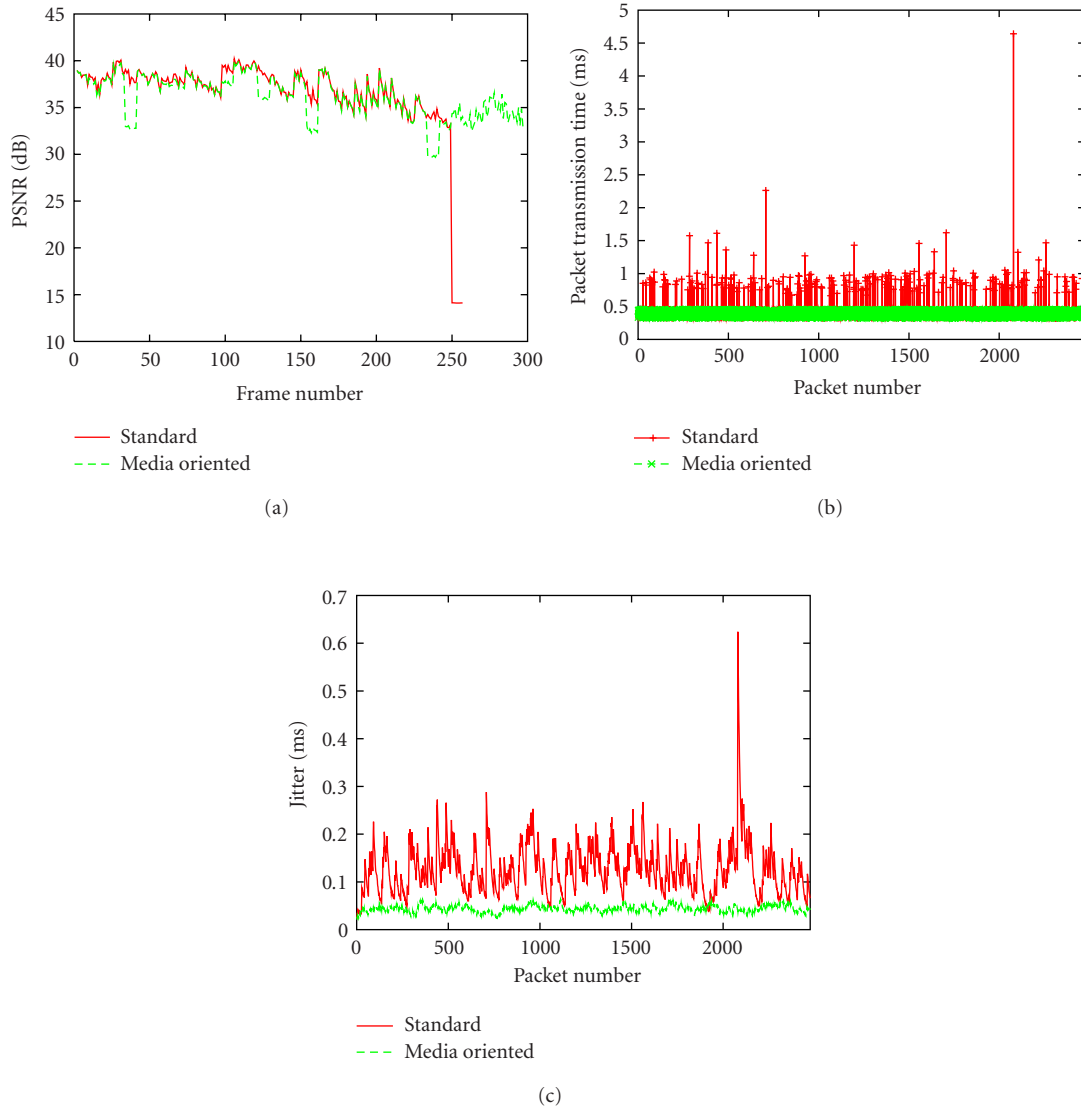
(a)

(b)

(c)

FIGURE 18: PSNR, transmission delay, and jitter comparison (SNR = 8.5 dB, 36 Mbps, FEC= 3/4, 16 QAM).

ence for ad hoc networks. For these simulations, 20 nodes are distributed in an area of 500×100 meters which is 9 times smaller than previous simulation scenarios. In this simulation, 6 UDP connections are set up between 12 different nodes. Data is generated by CBR sources at a saturation rate. The first source starts data transmission at time 3 : 12 and the last one at 25 : 12. For this simulation, nodes are fixed and DSR does not need to use *route maintenance*. The results are averaged over 30 different scenario patterns. Figure 14 shows the performance of MORSA in these experiments. Clearly, MORSA outperforms the standard mode selection (RBAR) and hybrid mode selection (H-MORSA) mechanisms. This is because the media-oriented mechanism considers the application's characteristics and does not use FEC at the physical layer when the channel condition is good.

6. EVALUATION OF VIDEO QUALITY

Simulation results in NS-2 have shown a significant improvement in throughput when considering the loss requirements of the application to select the transmission mode. In this section, we evaluate the effectiveness of the proposed media-oriented mechanism using the simulation of a video transmission over a 802.11a wireless channel. Our previous observations about the performance of the media-oriented mechanism can be further justified by the evaluation of the video quality obtained at the receiver when we employ the media-oriented mechanism. In the following sections, we describe a wireless channel model that can estimate the position and the length of burst error bits in 802.11a. Then, we present a video application that can tolerate a BER equal to 10^{-3} by using an application-level FEC
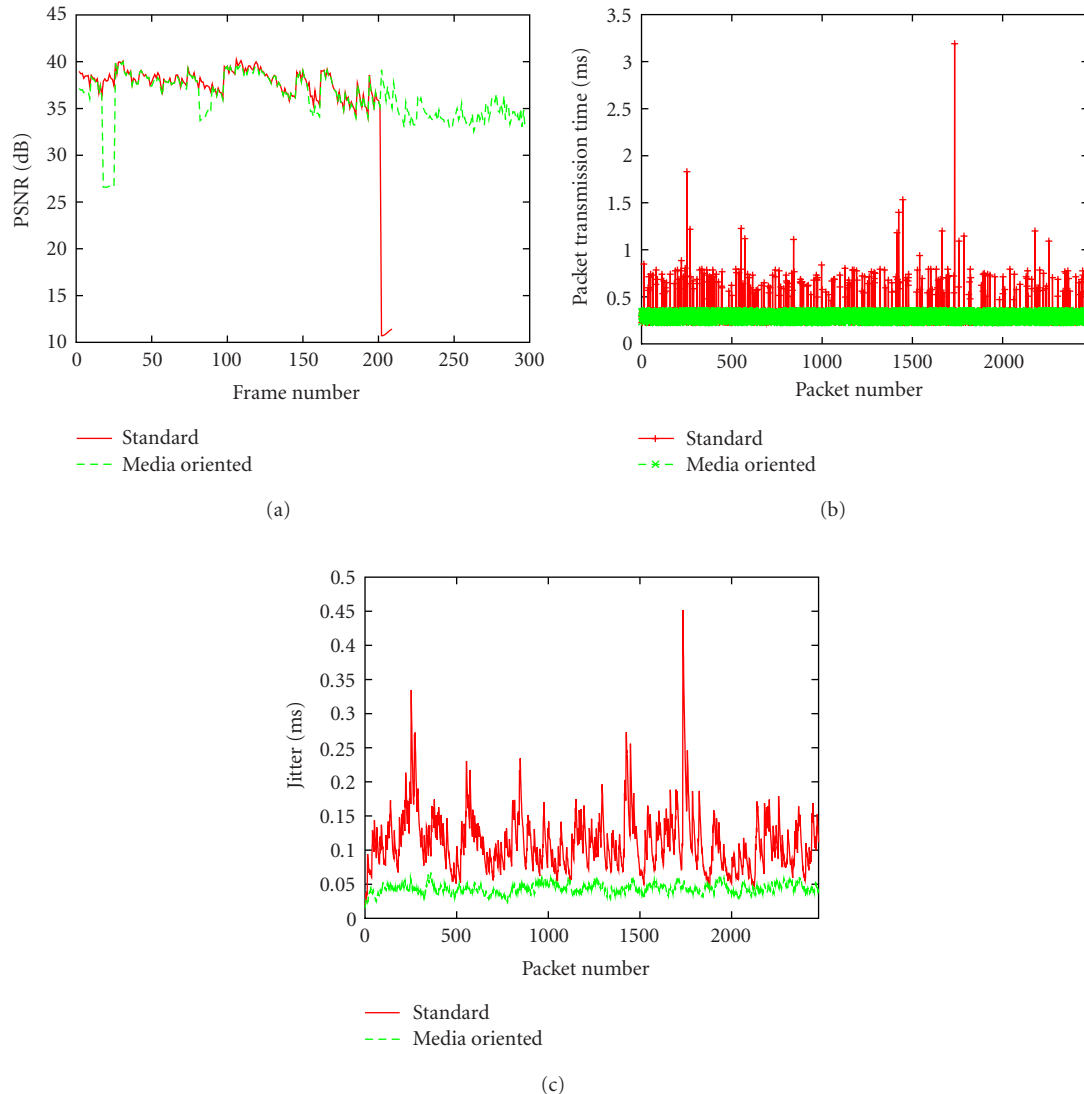
(a)

(b)

(c)

Figure 19: PSNR, transmission delay, and jitter comparison (SNR = 17.3 dB, 54 Mbps, FEC= 3/4, 64 QAM).

whose overhead is only 5%. Finally, we compare the transmission delay and the video quality (peak signal-to-noise ratio) with standard and media-oriented transmission mechanisms.

6.1. 802.11a channel model

Wireless channel models can be divided into two main groups: *memoryless models* and *models with memory*. In memoryless models, corrupted bits are produced by a sequence of independent trials. Each trial has the same probability p of producing a correct bit and probability $q = 1 - p$ of producing a bit error. However, in a real communication environment, links have memory and errors often occur in isolated bursts because of multipath fading, impulsive noise, or switch transients. A classic method to model a wireless channel with memory is using a Markov chain. In this model, the probability of bit error depends on the state of

the model. We have considered in this section a model with memory, which is based on the model proposed in [29] for 802.11a WLANs.

In the 802.11a physical layer, the data field will be encoded with a standard convolutional encoder of different coding rate $R = 1/2$, 2/3, or 3/4, depending on the data rate. The 1/2 convolutional encoder uses the generator polynomials $G_0 = 133_8$ and $G_1 = 171_8$ and simple puncturing is applied to derive higher convolutional rates [30]. Regarding convolutional decoding, it is usually implemented using the Viterbi algorithm.

In this paper, we use the derivation for distribution of error events obtained in these convolutional codes at the output of the Viterbi decoder. We estimate the position and the length of bit errors at the output of the decoder with this method. We use asymptotic bounds to analyze the distribution of error event lengths at the output of the
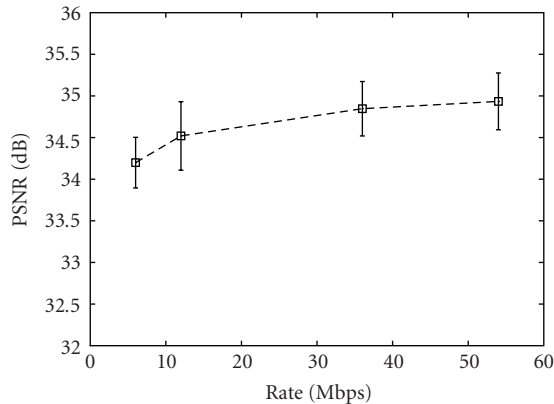
FIGURE 20: 95% confidence intervals of PSNR for different transmission modes with media-oriented mode selection mechanism.

Viterbi decoder. We also consider the relationship between the error probability of a random convolutional code and the error probability of a particular block code (termed *code termination* technique is presented in [31]). The tail of the distribution that is otherwise difficult to estimate with classical techniques can be estimated with this method.

Then, we use the error event length distribution and the distribution of errorless periods to derive a simple model which describes the residual error at the output of the soft-decision Viterbi decoder. In the next section, we use this model to compute the distribution of corrupted bits for different transmission modes.

6.2. Video encoder

The concept of fine-grain scalability (FGS) has been introduced in order to allow for dynamic rate adaptation to varying bandwidth and receiver capabilities. Compression solutions based on motion-compensated spatiotemporal signal decomposition have thus gained attention as viable alternatives to classical predictive techniques for scalable video representation. The video codec that has been used in the experiments reported here, referred to as WAVIX in the sequel, has been developed in this framework. Figure 15 shows the structure of WAVIX video encoder.

A group of frames (GOF) is fed into the coding system. In order to fine tune the bit rate allocated to the motion fields, the block-matching motion estimation makes use of a rate-constrained adaptive tree structure. The block size is thus adapted to local motion characteristics in a rate-distortion sense. The rate here refers to the bit rate allocated to encode the motion vectors and the distortion relates to the prediction error. The estimation itself, to save computation time, relies on a hierarchical approach. The motion vectors obtained in the first steps of the quadtree are used to initialize the search in the subsequent steps. The motion vectors are then predictively coded. The predictor is given by the median value of neighboring vectors. The prediction error is then coded using Huffman codes.

The GOF is fed to the motion-compensated temporal transform which is based on a two-taps Haar wavelet transform. The temporal decomposition is applied iteratively on pairs of images within the GOF. The advantage of the Haar wavelet transform is to achieve a fairly good temporal energy compaction with a limited number of motion fields (8 motion fields for a 3-stage temporal decomposition of a group of 8 images).Each temporal subband is then further decomposed by a biorthogonal 9-7 wavelet filter in the horizontal and vertical direction. In the experiments, 3-levels decomposition are being used. The subbands resulting from the spatiotemporal decomposition are then quantized with a uniform quantizer and encoded with a context-based bit-plane arithmetic coding as used in the JPEG-2000 standard [32]. The algorithm optimizing the truncation points in a rate-distortion sense handles groups of spatiotemporal subbands. The truncation point rate-distortion optimization leading to quality layers is well suited to fine tune the rate allocated to the texture information, hence to support fine-grain scalability.

An inter-GOF temporal prediction is also used as an option in the above coding system. The inter-GOF temporal prediction leads to GOFs of type intra and of type inter. The inter-GOF temporal prediction requires one additional motion field. This temporal prediction and corresponding motion estimation are realized in a closed loop. The closed-loop prediction is done by taking as reference information the corresponding image coded at a lower rate, as used in a base layer of a scalable representation. A more detailed description of this video codec can be found in [33].

Arithmetic codes are widely used in coding systems due to their high compression efficiency. They are however very sensitive to bit errors. A single bit error may lead to a complete desynchronization of the decoder. In order to make the WAVIX codec robust to errors, an error-resilient arithmetic codes decoding technique [34] has been integrated in the video decoder. The technique consists in exploiting the residual redundancy in the bitstream by using soft-decision decoding procedures. The term *soft* here means that the decoder takes in input and supplies not only binary (*hard*) decisions but also a measure of confidence (a probability) on the bits. One can thus exploit the so-called *excess rate* (or sub-optimality of the code), to reduce the catastrophic *desynchronization* effect of VLC decoders, hence to reduce the

(a)

(b)

FIGURE 21: A sample of video stream at the receiver, (a) transmitted by media-oriented algorithm with 0.1% bit errors (SNR= 1.3, rate = 12 Mbps), (b) original video stream.

residual symbol error rates. This amounts to exploiting inner codeword redundancy as well as the remaining correlation within the sequence of symbols (remaining inter symbol dependency).

In practice, the decoding algorithm can be regarded as a soft-input soft-output sequential decoding technique run on a tree. The complexity of the underlying Bayesian estimation algorithm growing exponentially with the number of coded symbols, a simple, yet efficient, pruning method is integrated. It allows the user to limit the complexity within a tractable and a realistic range, at a limited cost in terms of estimation accuracy.

In order to increase the resynchronization capability, a *soft synchronization* mechanism has been added. This mechanism relies on both the use of *soft synchronization* markers and of forbidden symbols. The *soft synchronization* markers are patterns, inserted in the symbol stream at some known positions, which serve as anchors for favoring the likelihood of correctly synchronized decoding paths. This *soft synchronization* idea augments the autosynchronization power of the chain at a controllable loss in information rate. The forbidden symbols, when used, provide additional error detection and correction capability [35].

The bitstream generated by WAVIX is split into motion vectors and texture. The texture is encoded with the EBCOT algorithm. Hence, it has the same properties as a JPEG-2000 bitstream. The corresponding bitstream is separated into header and entropy-coded data. The header contains high-level information, like GOF sizes, and provides a description of the structure of the entropy-coded data. As this information is essential to the decoder, it is protected by a Reed-Solomon block code with high redundancy (e.g., 127/255).

6.3. Multimedia transmission over 802.11a wireless channel

In this section, we evaluate the quality of the video bitstream at the receiver side when the media-oriented mechanism is used. In our experiments, the WAVIX video encoder is configured to encode a sample of 300 CIF video frames. The video bit rate is 2 Mps and each frame is a YUV image.[7] The number of frames in each GOF is 8. The activation of the WAVIX error resilience options corresponds to the addition of a 127/255 Reed-Solomon block code for header protection and of synchronization markers as explained in Section 6.2. The overhead of the header protection represents about 5.2% of the video stream while the overhead of the synchronization markers is negligible.

The transmission delay is calculated by considering the number of retransmissions and the value of the backoff timer [10]. The retransmission limit is defined in the IEEE 802.11 MAC standard specification with the help of the two following counters: the short retry count

(SRC) and the long retry count (LRC). These counters are incremented and reset independently. The SRC is incremented every time an RTS fails and LRC is incremented when data transmission fails. Both the SRC and the LRC are reset to 0 after a successful data transmission. Data frames are discarded when SRC (LRC) reaches dot11ShortRetryLimit (dot11LongRetryLimit). The default values for dot11ShortRetryLimit and dot11LongRetryLimit are 7 and 4, respectively.

Furthermore, we consider the backoff timer period after each retransmission. For each retransmission, we select a random backoff which is drawn from a uniform distribution over the interval $[0, CW]$. In each retransmission, CW is updated to either $2 \times (CW + 1) - 1$ or its maximal value aCW_{max}. Let $\bar{T}_{backoff}(i)$ denote the average backoff interval after i consecutive unsuccessful transmission attempts. It can be calculated by [36]

$$\bar{T}_{backoff}(i) = \begin{cases} \dfrac{2^i(aCW_{min}+1)-1}{2} \cdot aSlotTime, & 0 \le i \le 6, \\ \dfrac{aCW_{max}}{2} \cdot aSlotTime, & i \ge 6, \end{cases}$$

(5)

where aCW_{min}, aCW_{max}, and $aSlotTime$ are 15, 1023, and 9 microseconds for IEEE 802.11a WLANs [30].

We have chosen 4 SNRs corresponding to 4 different transmission modes (see Table 2). Using the 802.11a channel model described in Section 6.1, we can find the distribution of bit errors for each SNR and transmission mode at the output of Viterbi decoder. The bit errors are distributed over the packets of length 1000 bytes.

In the standard transmission mode, we only accept packets without corrupted bits. The error resilience options of the application layer are not employed for the standard transmission mechanism. However, we activate the WAVIX error resilience options and we accept packets with corrupted payload for the media-oriented mode selection mechanism.

Figures 16, 17, 18, and 19 show the PSNR, transmission delay, and interval jitter performance for 4 transmission modes with both the standard and the media-oriented mechanisms. Table 4 also shows the overall duration of the transmission for this video stream. As expected, the media-oriented mechanism (with LT = 0.1% and 5.2% FEC overhead at the application layer) significantly decreases the overall duration of the transmission (see Table 4).

We made the following observations from Figures 16, 17, 18, and 19. The packet transmission time is almost fixed with the media-oriented mechanism while it continuously changes with the number of retransmissions using the standard mechanism. When the media-oriented mechanism is used, the PSNR of the decoded video is equivalent to the standard transmission mode, except for the *drops* that correspond to GOFs where errors occur. In this case, error resilience options allow us to decode the GOFs with the best achievable visual quality. The corrupted frames exhibit a lower quality, but their visual content is preserved. When the

---

[7] The foreman CIF (352 × 288 pixels) video sequence has been used.

TABLE 4: Transmission time comparison for video transmission with and without media-oriented mechanism.

Modulation	Data rate (Mbps)	FEC rate	SNR (dB)	Transmission duration for standard (s)	Transmission duration for media oriented (s)
BPSK	6	1/2	−1.6	8.00	6.92
QPSK	12	1/2	1.3	4.14	3.57
16 QAM	36	3/4	8.5	1.09	0.96
64 QAM	54	3/4	17.3	0.81	0.72

PSNR remains above 30 dB, the degradation is generally unnoticeable for a human viewer. When the PSNR falls as low as 25 dB, the decoded frames are severely degraded but are still acceptable by a human viewer. The impact of errors on the visual quality depends on the characteristics of the current frame (in particular, the number and positions of errors, and the video content). In applications involving real-time constraints, as for instance visiophony or streaming, it may be preferable to receive a degraded frame rather than losing it entirely or slowing down the video playback because of packets retransmission.

Another observation from the PSNR calculation is that after 4 consecutive retransmissions, (i.e., when a packet is lost for good), the standard transmission mechanism cannot decode the rest of the video frame (e.g., this occurs at the frame number 220 in Figure 16). However, this problem can be solved at the transmitter side with a more intelligent packetization scheme, or by adding resynchronization patterns within the data flow. Nonetheless, in case of packet drop, the visual content of a full GOF may be lost.

Figures 16, 17, 18, and 19 also show the jitter for the standard and the media-oriented mode selection mechanisms. First, it is obviously and logically correlated to transmission delay. In the media-oriented mechanism, the jitter is much less important than with the standard mode. This is a very desirable property in the case of video transmission. Having a constant time interval between packets arrivals is equivalent to having a constant time slot available to decode each GOF. Therefore, complexity can be managed easily without the need for excessive buffering.

We have simulated the same scenarios for 10 different channel characteristics (different distributions of corrupted bits over data flow) in order to calculate the confidence interval of the PSNR with the media-oriented transmission mode. For each transmission rate, the 95% confidence intervals on the mean PSNR are computed. The intervals for the various rates are displayed by horizontal lines as shown in Figure 20. The results show an acceptable PSNR in all transmission modes. Figure 21 shows a sample of video stream transmitted with the media-oriented algorithm at 12 Mbps.

7. CONCLUSION

In this paper, we have presented a novel cross-layer mechanism in MANETs to select the best transmission mode which takes into account some characteristics of the application. This mechanism, which we believe to be easy to implement in actual devices, uses information from the physical channel and the loss tolerance requirements of the application to select the optimal PHY rate, modulation, and FEC transmission parameters. We have proposed new transmission modes which do not use FEC and which significantly increase the application throughput. NS-based simulation results in ad hoc networks show that our mechanism achieves up to 4 Mbps increase in throughput in MANETs. The gain obtained from the application point of view has been evaluated with the help of the WAVIX video encoder, which can tolerate a BER equal to 10^{-3} with only 5% of FEC overhead at the application level. The results show significant improvements in throughput, latency, and jitter.

REFERENCES

[1] S. Shakkottai, T. S. Rappaport, and P. C. Karlsson, "Cross-layer design for wireless networks," *IEEE Commun. Mag.*, vol. 41, no. 10, pp. 74–80, 2003.

[2] S. Toumpis, "Capacity and cross-layer design of wireless Ad Hoc networks," Ph.D. thesis, Department of Electrical Engineering of Stanford University, Stanford, Calif, USA, July, 2003.

[3] A. Safwat, H. Hassanein, and H. Mouftah, "Optimal cross-layer designs for energy-efficient wireless Ad Hoc and sensor networks," in *Proc. 22nd IEEE International Performance, Computing, and Communications Conference (IPCCC '03)*, pp. 123–128, Phoenix, Ariz, USA, April 2003.

[4] W. H. Yuen, H.-N. Lee, and T. D. Andersen, "A simple and effective cross layer networking system for mobile Ad Hoc networks," in *Proc. 13th IEEE International Symposium on Personal, Indoor and Mobile Radio Communications (PIMRC '02)*, vol. 4, pp. 1952–1956, Lisbon, Portugal, September 2002.

[5] G. Holland and N. Vaidya, "Analysis of TCP performance over mobile Ad Hoc networks," *Wireless Networks*, vol. 8, no. 2, pp. 275–288, 2002.

[6] J. Mitola, "The software radio architecture," *IEEE Commun. Mag.*, vol. 33, no. 5, pp. 26–38, 1995.

[7] H. Jegou and C. Guillemot, "Source multiplexed codes for error-prone channels," in *Proc. IEEE International Conference*

on Communications (ICC '03), vol. 5, pp. 3604–3608, Anchorage, Alaska, USA, May 2003.

[8] T. Guionnet, "Codage robuste par descriptions multiples pour transmission sans fil d'information multimédia," Ph.D. thesis, University of Rennes, Rennes Cedex, France, 2003.

[9] IEEE 802.11 WG, "Draft Supplement to STANDARD FOR Telecommunications and Information Exchange Between Systems-LAN/MAN Specific Requirements - Part 11: Wireless Medium Access Control (MAC) and Physical Layer (PHY) specifications: Medium Access Control (MAC) Enhancements for Quality of Service (QoS)," *IEEE 802.11e/Draft 4.2*, February 2003.

[10] IEEE 802.11 WG, "Wireless LAN Medium Access Control (MAC) and Physical Layer (PHY) specifications," *Standard Specification*, IEEE, 1999.

[11] A. Kamerman and L. Monteban, "WaveLAN-II: a highperformance wireless LAN for the unlicensed band," *Bell Labs Technical Journal*, vol. 2, no. 3, pp. 118–133, 1997.

[12] G. Holland, N. H. Vaidya, and P. Bahl, "A rate-adaptive MAC protocol for multi-hop wireless networks," in *Proc. ACM International Conference on Mobile Computing and Networking (MobiCom '01)*, pp. 236–251, Rome, Italy, July 2001.

[13] D. Qiao, S. Choi, A. Jain, and K. G. Shin, "MiSer: an optimal low-energy transmission strategy for IEEE 802.11 a/h," in *Proc. ACM International Conference on Mobile Computing and Networking (Mobicom '03)*, pp. 161–175, San Diego, Calif, USA, September 2003.

[14] V. Bhuvaneshwar, M. Krunz, and A. Muqattash, "CONSET: a cross-layer power aware protocol for mobile Ad Hoc networks," in *Proc. IEEE International Conference on Communications (ICC '04)*, pp. 4067–4071, Paris, France, June 2004.

[15] U. C. Kozat, I. Koutsopoulos, and L. Tassiulas, "A framework for cross-layer design of energy-efficient communication with QoS provisioning in multi-hop wireless networks," in *Proc. 23rd IEEE Annual Joint Conference of Computer and Communications Societies (INFOCOM '04)*, vol. 2, pp. 1446–1456, Hong Kong, China, March 2004.

[16] S. Krishnamachari, M. VanderSchaar, S. Choi, and X. Xu, "Video streaming over wireless LANs: a cross-layer approach," in *Proc. IEEE Packet Video 2003 (PV '03)*, Nantes, France, April 2003.

[17] M. Conti, G. Maselli, G. Turi, and S. Giordano, "Cross-layering in mobile Ad Hoc network design," *IEEE Computer*, vol. 37, no. 2, pp. 48–51, 2004.

[18] Y. Shan and A. Zakhor, "Cross layer techniques for adaptive video streaming over wireless networks," in *Proc. IEEE International Conference on Multimedia and Expo (ICME '02)*, vol. 1, pp. 277–280, Lausanne, Switzerland, August 2002.

[19] H. Liu and M. El Zarki, "Adaptive source rate control for real-time wireless video transmission," *Mobile Networks and Applications*, vol. 3, no. 1, pp. 49–60, 1998.

[20] M. Pursley and D. Taipale, "Error probabilities for spread-spectrum packet radio with convolutional codes and Viterbi decoding," *IEEE Trans. Commun.*, vol. 35, no. 1, pp. 1–12, 1987.

[21] P. Frenger, "Multi-rate codes and multicarrier modulation for future communication system," Ph.D. thesis, Chalmers University of Technology, Goteborg, Sweden, 1999.

[22] Q. Ni, L. Romdhani, and T. Turletti, "A Survey of QoS enhancements for IEEE 802.11 wireless LAN," *Journal of Wireless Communication and Mobile Computing*, vol. 4, no. 5, pp. 547–566, 2004.

[23] M. H. Manshaei, T. Turletti, and M. Krunz, "A media-oriented transmission mode selection in 802.11 wireless LANs," in *Proc. IEEE Wireless Communications and Networking Confer-*

ence (WCNC '04), vol. 2, pp. 1228–1233, Atlanta, Ga, USA, March 2004.

[24] L. A. Larzon, M. Degermark, and S. Pink, "UDP lite for real time applications," Tech. Rep. 1999-01, HP Laboratories Bristol, Bristol, UK, April 1999.

[25] M. H. Manshaei and T. Turletti, "Simulation-based performance analysis of 802.11a wireless LAN," in *Proc. International Symposium on Telecommunications (IST '03)*, Isfahan, Iran, August 2003.

[26] "The Rice University Monarch Project, Mobile Networking Architectures," http://www.monarch.cs.rice.edu/.

[27] "Cisco Aironet 1200 Series Access Point Hardware Installation Guide," available in http://www.cisco.com.

[28] D. B. Johnson, D. A. Maltz, and J. Broch, "DSR: the dynamic source routing protocol for multi-hop wireless Ad Hoc networks," in *Ad Hoc Networking*, C. E. Perkins, Ed., chapter 5, pp. 139–172, Addison-Wesley, Boston, Mass, USA, 2001.

[29] R. Khalili and K. Salamatian, "A new analytic approach to evaluation of packet error rate in wireless networks," Research Report RP-LIP6-2004-10-50, LIP6-CNRS, October 2004.

[30] IEEE 802.11 WGPart 11a, "Wireless LAN medium access control (MAC) and physical Layer (PHY) specifications," High-speed Physical Layer in the 5 GHz Band, *Standard Specification*, IEEE, 1999.

[31] G. D. Forney Jr., "Convolutional codes II. Maximum-likelihood decoding," *Information and Control*, vol. 25, no. 3, pp. 222–266, 1974.

[32] D. S. Taubman and M. W. Marcellin, *JPEG2000: Fundamentals, Standards and Practice*, Kluwer Academic, Boston, Mass, USA, 2002.

[33] J. Vieron and C. Guillemot, "Low rate FGS video compression based on motion-compensated spatio-temporal wavelet analysis," in *International Conference on Visual Communication and Image Processing (VCIP '03)*, Proc. SPIE, pp. 732–744, Lugano, Switzerland, July 2003.

[34] T. Guionnet and C. Guillemot, "Soft decoding and synchronization of arithmetic codes: application to image transmission over noisy channels," *IEEE Trans. Image Processing*, vol. 12, no. 12, pp. 1599–1609, 2003.

[35] I. Kozintsev, J. Chou, and K. Ramchandran, "Image transmission using arithmetic coding based continuous error detection," in *Proc. Data Compression Conference (DCC '98)*, pp. 339–348, Snowbird, Utah, USA, March–April 1998.

[36] D. Qiao and S. Choi, "Goodput enhancement of IEEE 802.11a wireless LAN via link adaptation," in *Proc. IEEE International Conference on Communications (ICC '01)*, vol. 7, pp. 1995–2000, Helsinki , Finland, June 2001.

Mohammad Hossein Manshaei received his B.S. degree in electrical engineering and his M.S. degree in communication engineering from the Isfahan University of Technology (IUT), Iran, in 1997 and 2000, respectively. He joined as a Research Assistant at the Department of Electrical and Computer Engineering in IUT in July 2000. He received another M.S. degree in computer science from the University of Nice Sophia Antipolis in 2002. He is currently pursuing his Ph.D. degree in computer science in the Planète group at INRIA Sophia Antipolis. His research interests include wireless networking and adaptive communication protocols.

Thierry Turletti received the M.S. (1990) and the Ph.D. (1995) degrees in computer science both from the University of Nice Sophia Antipolis, France. During his Ph.D. studies in the RODEO Group at INRIA Sophia Antipolis, he designed one of the first videoconferecening tool for the Internet. From 1995 to 1996, he was a post-doctoral Fellow in the Telemedia, Networks, and Systems Group at Laboratory for Computer Science (LCS), Massachusetts Institute of Technology (MIT). He is currently a full-time Researcher in the Planète Group at INRIA Sophia Antipolis. His research interests include multimedia applications, multicast transmission, and wireless networking. He currently serves on the Editorial Board of Wireless Communications and Mobile Computing.

Thomas Guionnet received the B.S. degree from the University of Newcastle upon Tyne, UK, in computer science, in 1997. He obtained the Engineer degree in computer science and image processing and the Ph.D. degree from the University of Rennes 1, France, respectively, in 1999 and 2003. He was a Research Engineer at INRIA from 2003 to 2004 and was involved in the French National Project RNRT VIP and in the JPEG-2000 Part 11—JPWL Ad hoc Group. He is currently a Research Engineer at Envivio and is involved in the design of high-performance real-time MPEG4-AVC/H.264 encoder. His research interests include image processing, coding, and joint source and channel coding.